CHAPTER 6

# STUDY OF HEAT AND MASS TRANSFER IN UNSTEADY TWO DIMENSIONAL NANOFLUID FLOW BETWEEN PARALLEL PLATES

Content of this chapter is communicated.

# Chapter 6

## STUDY OF HEAT AND MASS TRANSFER IN UNSTEADY TWO DIMENSIONAL NANOFLUID FLOW BETWEEN PARALLEL PLATES

In previous chapter, it is assumed that the concentration of fluid particles is uniform. But, in many real problems involving convection of nanofluids, mechanism such as thermophoresis and Brownian motion are evident, the concentration of nanofluids may not be considered as uniform. In this chapter, influence of magnetic field on two dimensional squeezing nanofluid flow considering heat and mass transfer between two plates is examined.

## 6.1 Introduction

Exploration of heat and mass transfer for time dependent squeezing viscous flow between two parallel plates, is vital in engineering such as cooling towers, damage of crops due to freezing, chemical processing equipment, formation and dispersion of fog and food processing. Sheikholeslami et al. [76] studied unsteady nanofluid flow between parallel plates using Differential Transformation Method.

Sheikholeslami et al. [74] considered two phase model to simulate the problem of unsteady nanofluid flow between parallel plates. Hatami et al. [16] examined unsteady squeezing nanofluid flow between parallel plates in presence of variable magnetic field. Sheikholeslami et al. [71] discussed unsteady squeezing nanofluid flow and heat transfer, taking various nanoparticles in the study, but uniform mass distribution was considered. Usman et al. [112] extended above work by considering both heat and mass transfer characteristics.

## 6.2 Novelty of the Problem

The objective of this study is to scrutinize impact of magnetic field and thermal radiation on nanofluid flow through squeezing parallel plates. Novelty of the present work is the inclusion of effects of thermal interfacial resistance and Brownian motion on thermal conductivity along with micro mixing in suspensions. The simplified system of ODE is solved using HAM. Effects

of relevant parameters are discussed. In most of the studies, the concentration of fluid particles is considered to be uniform, but slips mechanism such as Brownian motion and thermophoresis are always evident in convection of nanofluids. These phenomenon are considered in present study.

## 6.3 Mathematical Formulation of the Problem

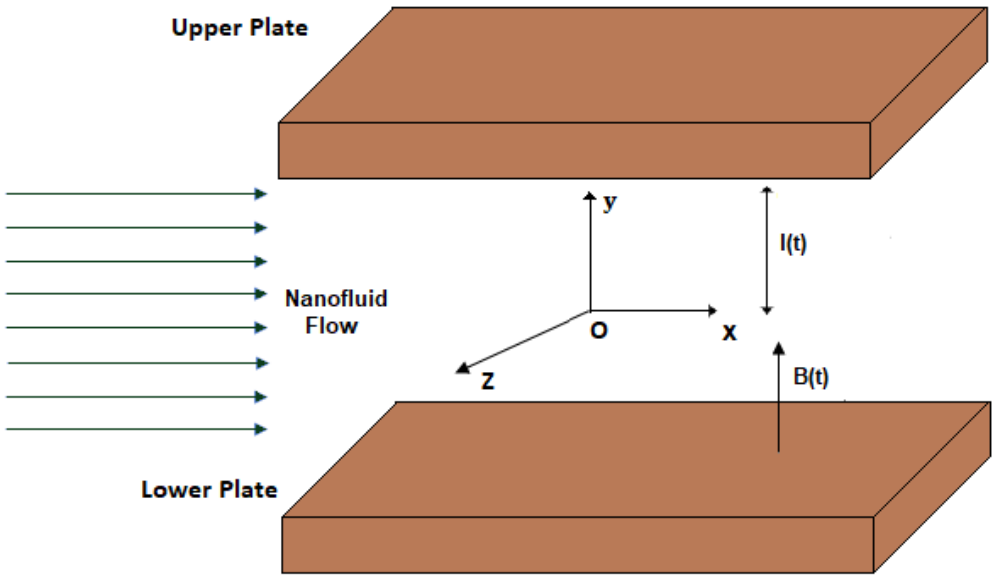


**Figure 6.1**: Physical Sketch of the Problem

Fluid under consideration is $Al_2O_3$ − water nanofluid. A coordinate system is chosen as shown in Figure 6.1. Squeezing flow is supposed to be between two horizontal parallel moving plates situated at $l(t) = L(1 - at)^{1/2}$units apart. Here $L$ is the initial position of the plate, $a > 0$ signifies that plates are squeezed until they touch each other at $t = \frac{1}{a}$ and plates move in opposite direction for $a < 0$. A uniform magnetic flux with density $B(t) = B/\sqrt{1 - at}$ ($B$ is the initial value) is applied.

Under these assumptions, governing equations are:

$$\frac{\partial u}{\partial x} + \frac{\partial v}{\partial y} = 0, \tag{6.1}$$

$$\rho_{nf}\left(\frac{\partial u}{\partial t}+u\frac{\partial u}{\partial x}+v\frac{\partial u}{\partial y}\right)=\mu_{nf}\left(\frac{\partial^2 u}{\partial x^2}+\frac{\partial^2 u}{\partial y^2}\right)-\sigma_{nf}B^2(t)u, \tag{6.2}$$

$$\rho_{nf}\left(\frac{\partial v}{\partial t}+u\frac{\partial v}{\partial x}+v\frac{\partial v}{\partial y}\right)=\mu_{nf}\left(\frac{\partial^2 v}{\partial x^2}+\frac{\partial^2 v}{\partial y^2}\right), \tag{6.3}$$

$$\frac{\partial T}{\partial t}+u\frac{\partial T}{\partial x}+v\frac{\partial T}{\partial y}=\frac{k_{nf}}{(\rho c_p)_{nf}}\left(\frac{\partial^2 T}{\partial x^2}+\frac{\partial^2 T}{\partial y^2}\right)+\frac{\mu_{nf}}{(\rho c_p)_{nf}}\left(2\left[\left(\frac{\partial u}{\partial x}\right)^2+\left(\frac{\partial v}{\partial y}\right)^2\right]+\left(\frac{\partial u}{\partial y}+\frac{\partial v}{\partial x}\right)^2\right)$$

$$+\frac{(\rho c_p)_s}{(\rho c_p)_f}\left(\frac{D_T}{T_w}\left(\left(\frac{\partial T}{\partial x}\right)^2+\left(\frac{\partial T}{\partial y}\right)^2\right)+D_B\left(\frac{\partial C}{\partial x}\frac{\partial T}{\partial x}+\frac{\partial C}{\partial y}\frac{\partial T}{\partial y}\right)\right)-\frac{1}{(\rho c_p)_{nf}}\frac{\partial q_r}{\partial y}+\frac{(\rho c_p)_{nf}Q(T-T_0)}{\rho_{nf}}, \tag{6.4}$$

$$u\frac{\partial C}{\partial x}+v\frac{\partial C}{\partial y}+w\frac{\partial C}{\partial z}=D_B\left(\frac{\partial^2 C}{\partial x^2}+\frac{\partial^2 C}{\partial y^2}+\frac{\partial^2 C}{\partial z^2}\right)+\frac{D_T}{T_w}\left(\frac{\partial^2 T}{\partial x^2}+\frac{\partial^2 T}{\partial y^2}+\frac{\partial^2 T}{\partial z^2}\right), \tag{6.5}$$

where

$$\rho_{nf}=(1-\emptyset)\rho_f+\emptyset\rho_s, \tag{6.6}$$

$$\sigma_{nf}=\sigma_f\left[1+\frac{3(\sigma-1)\emptyset}{(\sigma+2)-(\sigma-1)\emptyset}\right],\ \sigma=\frac{\sigma_s}{\sigma_f}, \tag{6.7}$$

$$\left(\rho c_p\right)_{nf}=(1-\emptyset)(\rho c_p)_f+\emptyset(\rho c_p)_s, \tag{6.8}$$

$$k_{nf}=k_f\left[1-3\frac{\emptyset(k_f-k_s)}{2k_f+k_s+\emptyset(k_f-k_s)}\right]. \tag{6.9}$$

Considering effects of micro mixing in suspensions on viscosity,

$$\mu_{nf}=\mu_{static}+\mu_{Brownian}=\frac{\mu_f}{(1-\emptyset)^{2.5}}+\frac{k_{Brownian}*\mu_f}{k_f*Pr_f}. \tag{6.10}$$

The thermo-physical properties of water and nanoparticles are as in Table 1.1.

$q_r$ [61] becomes:

$$q_r=-\frac{4\sigma^*}{3k^*}\frac{\partial T^4}{\partial y}=-\frac{4\sigma^*}{3k^*}\frac{\partial\left(4{T_0}^3T-3{T_0}^4\right)}{\partial y}. \tag{6.11}$$

Boundary conditions are

$$u\ =\ 0;\ v\ =\ \frac{dl}{dt};\ T\ =\ T_L;C=C_L\ at\ y=\ l(t), \tag{6.12}$$

$$\frac{\partial u}{\partial y} = 0;\ v\ =\ 0;\ \frac{\partial T}{\partial y} = 0; \frac{\partial C}{\partial y} = 0\ at\ y\ = 0. \tag{6.13}$$

Introducing non dimensional variables

$$\eta = \frac{y}{L(1-at)^{\frac{1}{2}}},\ u = \frac{ax}{2(1-at)} f'(\eta),\ v = \frac{-aL}{(1-at)^{\frac{1}{2}}} f(\eta),\ \theta(\eta) = \frac{\mathrm{T}}{T_L},\ C(\eta) = \frac{C}{C_L},$$

$$B(t) = \frac{B}{(1-at)^{1/2}}\ , \delta = \frac{L}{x}, \lambda = \frac{Q2L(T_L-T_0)(1-at)}{k_f T_L \rho_f}. \tag{6.14}$$

Therefore, dimensionless form of governing momentum, energy and mass transfer equations for this problem are given by:

$$a_1 f^{iv} - S(f'f'' + (-f+\eta)f''' + 3f'') - a_3 M^2 f'' = 0, \tag{6.15}$$

$$\theta'' + Pr\big(Sa_2(f-\eta)\theta' + Eca_4(4\delta^2 f'^2 + f''^2)\big) + NbC'\theta' + Nt\theta'^2 + a_2\theta\lambda = 0, \tag{6.16}$$

$$Nb\mathrm{C}'' + Nt\theta'' + S \cdot Nb \cdot Sc(fC' - \eta C'') = 0, \tag{6.17}$$

where

$$Pr = \frac{\mu_f \left(\rho c_p\right)_f}{\rho_f k_f}, \tag{6.18}$$

$$M^2 = \frac{\sigma_f a B^2 L^2}{\rho_f v_f}, \tag{6.19}$$

$$S = \frac{aL^2}{2v_f}, \tag{6.20}$$

$$Ec = \frac{\rho_f (ax)^2}{\left(\rho c_p\right)_f T_L 4(1-at)^2}, \tag{6.21}$$

$$b_0 = 1 - \emptyset, \tag{6.22}$$

$$b_1 = (b_0 + \emptyset \frac{\rho_s}{\rho_f}), \tag{6.23}$$

$$b_2 = \frac{1}{{b_0}^{2.5}}, \tag{6.24}$$

$$b_3 = (b_0 + \emptyset \frac{(\rho c_p)_s}{(\rho c_p)_f}), \tag{6.25}$$

$$b_4 = \frac{k_{nf}}{k_f}, \tag{6.26}$$

$$b_5 = \frac{\sigma_{nf}}{\sigma_f}, \tag{6.27}$$

$$a_1 = \frac{1}{{b_0}^{2.5} b_1}, \tag{6.28}$$

$$a_2 = \frac{b_3}{b_4 + Nr}, \tag{6.29}$$

$$a_3 = \frac{b_5}{b_1}, \tag{6.30}$$

$$a_4 = \frac{b_2}{b_4}, \tag{6.31}$$

$$Nr = \frac{16\sigma^* {T_0}^3}{3k^* k_f}, \tag{6.32}$$

subject to

$$f = 0, f'' = 0,\ \theta' = 0,\ C' = 0\ at\ \eta = 0, \tag{6.33}$$

$$f = 1, f' = 0,\ \theta = 1,\ C = 1\ at\ \eta = 1. \tag{6.34}$$

## 6.4 Solution by Homotopy analysis Method

Equations (6.15) – (6.17) subject to boundary conditions (6.33) – (6.34) are solved using Homotopy analysis method (HAM) [40].

Initial guess is:

$$f_0(\eta) = (3\eta - \eta^3)/2;\ \ \theta_0(\eta) = 1;\ C_0(\eta) = 1; \tag{6.35}$$

with auxiliary linear operators:

$$L_f = \frac{\partial^4 f}{\partial \eta^4}\ ,\ L_\theta = \frac{\partial^2 \theta}{\partial \eta^2}\ ,\ L_C = \frac{\partial^2 C}{\partial \eta^2}, \tag{6.36}$$

such that

$$L_f(C_1 + C_2\,\eta + C_3\eta^2 + C_4\eta^3) = 0,\ L_\theta(\,C_5 + C_6\eta) = 0,\ L_C(\,C_7 + C_8\eta) = 0, \tag{6.37}$$

where $c_1,\ \ c_2, \ldots, c_8$ are the arbitrary constants.

The zeroth order deformation problems are constructed as follows:

$$(1-p)L_f\left[\hat{f}(\eta;\ p)-f_0(\eta)\right]=p\hbar_f N_f\left[\hat{f}(\eta;\ p),\hat{\theta}(\eta;\ p),\hat{C}(\eta;\ p)\right], \tag{6.38}$$

$$(1-p)L_\theta\left[\hat{\theta}(\eta;\ p)-\theta_0(\eta)\right]=p\hbar_\theta N_\theta\left[\hat{f}(\eta;\ p),\hat{\theta}(\eta;\ p),\hat{C}(\eta;\ p)\right], \tag{6.39}$$

$$(1-p)L_C\left[\hat{C}(\eta;\ p)-C_0(\eta)\right]=p\hbar_C N_C\left[\hat{f}(\eta;\ p),\hat{\theta}(\eta;\ p),\hat{C}(\eta;\ p)\right], \tag{6.40}$$

subject to the boundary conditions:

$$\hat{f}(0;\ p)=0,\quad \hat{f}''(0;\ p)=0; \tag{6.41}$$

$$\hat{f}(1;\ p)=1,\quad \hat{f}'(1;\ p)=0; \tag{6.42}$$

$$\hat{\theta}'(0;\ p)=0,\quad \hat{\theta}(1;\ p)=1; \tag{6.43}$$

$$\hat{C}'(0;\ p)=0,\quad \hat{C}(1;\ p)=1. \tag{6.44}$$

The nonlinear operators are defined as

$$N_f\left[\hat{f}(\eta;\ p),\hat{\theta}(\eta;\ p),\hat{C}(\eta;\ p)\right]=\ a_1\frac{\partial^4\hat{f}}{\partial\eta^4}-S\left(\frac{\partial\hat{f}}{\partial\eta}\frac{\partial^2\hat{f}}{\partial\eta^2}+\left(-\hat{f}+\eta\right)\frac{\partial^3\hat{f}}{\partial\eta^3}+3\frac{\partial^2\hat{f}}{\partial\eta^2}\right)-a_3M^2\frac{\partial^2\hat{f}}{\partial\eta^2}, \tag{6.45}$$

$$N_\theta\left[\hat{f}(\eta;\ p),\hat{\theta}(\eta;\ p),\hat{C}(\eta;\ p)\right]=\frac{\partial^2\hat{\theta}}{\partial\eta^2}+Pr\left(Sa_2\left(\hat{f}-\eta\right)\frac{\partial\hat{\theta}}{\partial\eta}+Eca_4\left(4\delta^2\left(\frac{\partial\hat{f}}{\partial\eta}\right)^2+\frac{\partial^2\hat{f}^2}{\partial\eta^2}\right)\right)+$$

$$Nb\frac{\partial\hat{C}}{\partial\eta}\frac{\partial\hat{\theta}}{\partial\eta}+Nt\left(\frac{\partial\hat{\theta}}{\partial\eta}\right)^2+a_2\theta\lambda, \tag{6.46}$$

$$N_C\left[\hat{f}(\eta;\ p),\hat{\theta}(\eta;\ p),\hat{C}(\eta;\ p)\right]=Nb\frac{\partial^2\hat{C}}{\partial\eta^2}+Nt\frac{\partial^2\hat{\theta}}{\partial\eta^2}+SNbSc\left(\hat{f}\frac{\partial\hat{C}}{\partial\eta}-\eta\frac{\partial^2\hat{C}}{\partial\eta^2}\right), \tag{6.47}$$

where $\hat{f}(\eta;\ p)$, $\widehat{\theta}(\eta;\ p)$ and $\hat{C}(\eta;\ p)$ are unknown functions with respect to $\eta$ and $p$. $\hbar_f, \hbar_\theta$ and $\hbar_C$ are non-zero auxiliary parameters and $N_f$, $N_\theta$ and $N_C$ are nonlinear operators.

Also, $p\in(0,\ 1)$ is an embedding parameter. For $p=0$ and $p=1$,

$$\hat{f}(\eta;0)=f_0(\eta),\hat{f}(\eta;1)=f(\eta), \tag{6.48}$$

$$\hat{\theta}(\eta;0)=\ \theta_0(\eta),\hat{\theta}(\eta;1)=\ \theta(\eta), \tag{6.49}$$

$$\hat{C}(\eta;0)=\ C_0(\eta),\hat{C}(\eta;1)=\ C(\eta). \tag{6.50}$$

In other words, when variation of $p$ is taken from 0 to 1 then $\hat{f}(\eta;\ p), \hat{\theta}(\eta;\ p)$ and $\hat{C}(\eta;\ p)$ vary from $f_0(\eta), \theta_0(\eta)$ and $C_0(\eta)$ to $f(\eta), \theta(\eta)$ and $C(\eta)$ respectively. Taylor's series expansion of these functions yield the following:

$$\hat{f}(\eta;\ p) = f_0(\eta) + \sum_{m=1}^{\infty} f_m(\eta) p^m, \tag{6.51}$$

$$\hat{\theta}(\eta;\ p) = \theta_0(\eta) + \sum_{m=1}^{\infty} \theta_m(\eta) p^m, \tag{6.52}$$

$$\hat{C}(\eta;\ p) = C_0(\eta) + \sum_{m=1}^{\infty} C_m(\eta) p^m, \tag{6.53}$$

where

$$f_m(\eta) = \frac{1}{m!}\left[\frac{\partial^m f(\eta; p)}{\partial p^m}\right]_{p=0}, \tag{6.54}$$

$$\theta_m(\eta) = \frac{1}{m!}\left[\frac{\partial^m \theta(\eta; p)}{\partial p^m}\right]_{p=0}, \tag{6.55}$$

$$C_m(\eta) = \frac{1}{m!}\left[\frac{\partial^m C(\eta; p)}{\partial p^m}\right]_{p=0}. \tag{6.56}$$

It should be noted that the convergence in the above series strongly depends upon $\hbar_f, \hbar_\theta$ and $\hbar_C$. Assuming that these nonzero auxiliary parameters are chosen so that Equations (6.51) - (6.53) converge at $p = 1$. Hence, one can obtain the following:

$$f(\eta) = f_0(\eta) + \sum_{m=1}^{\infty} f_m(\eta), \tag{6.57}$$

$$\theta(\eta) = \theta_0(\eta) + \sum_{m=1}^{\infty} \theta_m(\eta), \tag{6.58}$$

$$C(\eta) = C_0(\eta) + \sum_{m=1}^{\infty} C_m(\eta). \tag{6.59}$$

Differentiating the zeroth order deformation (6.38) – (6.40) and (6.41) – (6.44) m times with respect to $p$ and substituting $p = 0$, and finally dividing by $m!$; the m$^{th}$ order deformation

$(m \geq 1)$ is

$$L_f[f_m(\eta) - \chi_m f_{m-1}(\eta)] = \hbar_f R_{f,m}(\eta), \tag{6.60}$$

$$L_\theta[\theta_m(\eta) - \chi_m\theta_{m-1}(\eta)] = \hbar_\theta R_{\theta,m}(\eta), \tag{6.61}$$

$$L_C[C_m(\eta) - \chi_m C_{m-1}(\eta)] = \hbar_C R_{C,m}(\eta), \tag{6.62}$$

subject to the boundary conditions

$$f_m(0) = f_m''(0) = 0, \tag{6.63}$$

$$f_m(1) = f_m'(1) = 0, \tag{6.64}$$

$$\theta_m(0) = \theta_m(1) = 0, \tag{6.65}$$

$$C_m'(0) = C_m(1) = 0, \tag{6.66}$$

with

$$R_{f,m}(\eta) = a_1 f_{m-1}^{iv} - S\left(\sum_{j=0}^{m-1} f_j' f_{m-1-j}'' - \sum_{j=0}^{m-1} f_j f_{m-1-j}''' + \eta f_{m-1}''' + f_{m-2}''' + 3f_{m-1}''\right) - a_3 M^2 f_{m-1}'', \tag{6.67}$$

$$R_{\theta,m}(\eta) = \theta_{m-1}'' + Pr\left(Sa_2\left(\sum_{j=0}^{m-1} f_j\theta_{m-1-j}' - \eta\theta_{m-1}' - \theta_{m-2}'\right) + Eca_4\left(4\delta^2 \sum_{j=0}^{m-1} f_j' f_{m-1-j}' + \sum_{j=0}^{m-1} f_j'' f_{m-1-j}''\right)\right) + Nb\sum_{j=0}^{m-1} C_j'\theta_{m-1-j}' + Nt\sum_{j=0}^{m-1}\theta_j'\theta_{m-1-j}' + a_2\lambda\theta_{m-1}, \tag{6.68}$$

$$R_{C,m}(\eta) = NbC_{m-1}'' + Nt\theta_{m-1}'' + SNbSc\left(\sum_{j=0}^{m-1} f_j C_{m-1-j}' - \eta C_{m-1}'' - C_{m-2}''\right), \tag{6.69}$$

where

$$\chi_m = \begin{cases} 0, & m \le 1 \\ 1, & m > 1 \end{cases}. \tag{6.70}$$

Solving the corresponding m[th] order deformation equations,

$$f_m(\eta) = f_m^*(\eta) + C_1 + C_2\,\eta + C_3\eta^2 + C_4\eta^3, \tag{6.71}$$

$$\theta_m(\eta) = \theta_m^*(\eta) + C_5 + C_6\eta, \tag{6.72}$$

$$C_m(\eta) = C_m^*(\eta) + C_7 + C_8\eta. \tag{6.73}$$

Here $f_m^*$ , $\theta_m^*$ and $C_m^*$ are given by are particular solutions of the corresponding m[th] order equations and constants $C_i(\ i = 1, 2, \dots, 8)$ are to be determined by the boundary conditions.

### 6.4.1 Convergence of solution

Figures 6.2 – 6.4 clearly suggest admissible range for auxiliary parameters $\hbar_f$, $\hbar_\theta$ and $\hbar_C$.

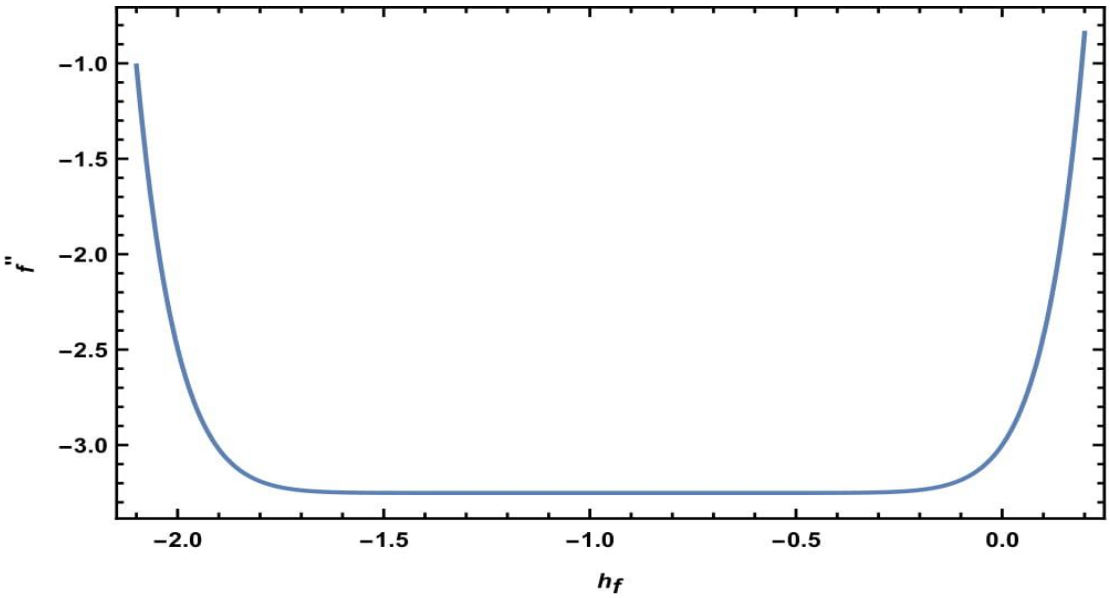


**Figure 6.2:** H-Curve of $f''$ for $\hbar_f$ at $\phi = 0.02,\ M = 0.5,\ Nr = 1.0, Pr = 10.0,\ S = 0.3,\ Ec = 0.05,\ \delta = 0.15,\ \lambda = 1.2,\ Nb = 0.1,\ Nt = 0.1\ and\ Sc = 0.3$.

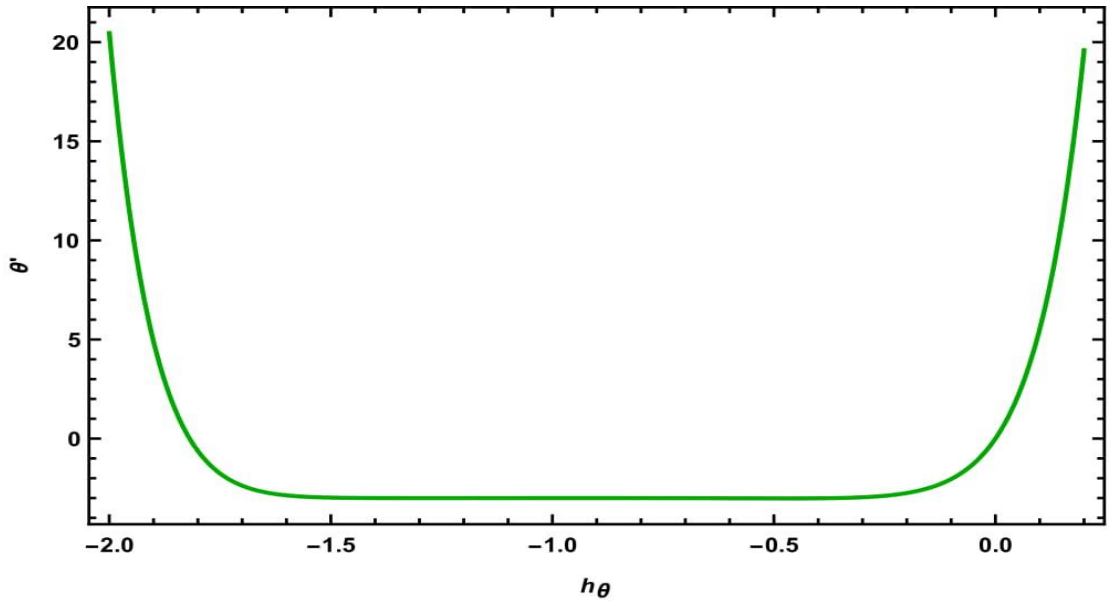


**Figure 6.3:** H-Curve of $\theta'$ for $\hbar_\theta$ at $\phi = 0.02,\ M = 0.5,\ Nr = 1.0, Pr = 10.0,\ S = 0.3,\ Ec = 0.05,\ \delta = 0.15,\ \lambda = 1.2,\ Nb = 0.1,\ Nt = 0.1\ and\ Sc = 0.3$.

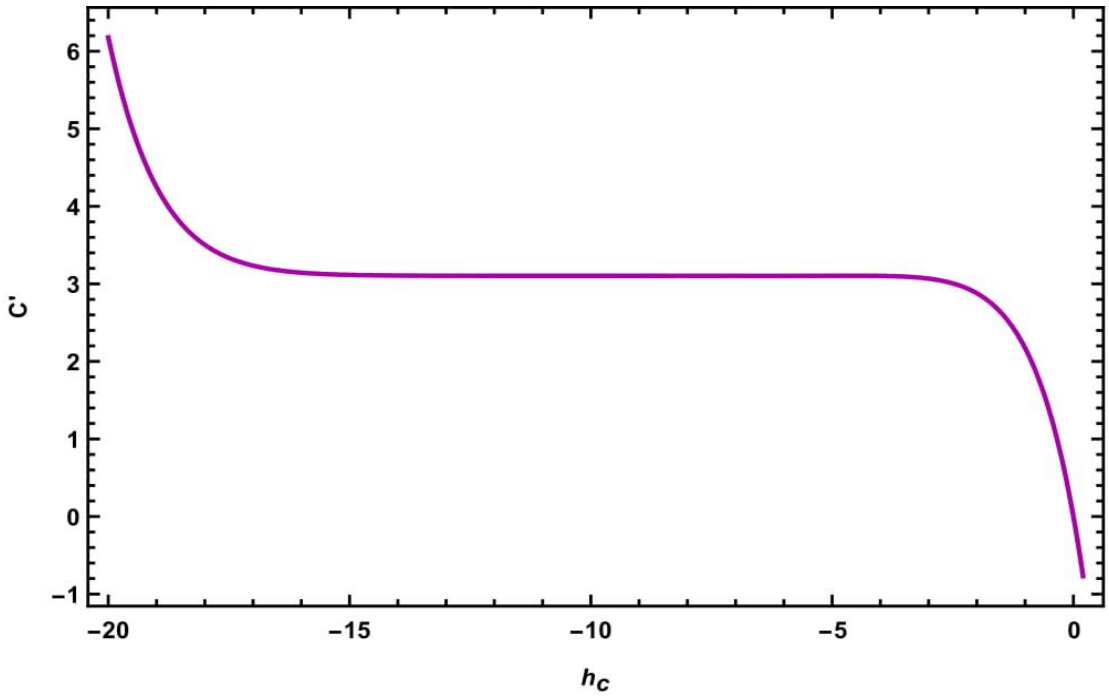


**Figure 6.4:** H-Curve of $C'$ for $\hbar_C$ at $\phi = 0.02,\ M = 0.5,\ Nr = 1.0, Pr = 10.0,\ S = 0.3,$ $Ec = 0.05,\ \delta = 0.15,\ \lambda = 1.2,\ Nb = 0.1,\ Nt = 0.1\ and\ Sc = 0.3.$

## 6.5 Results and Discussion

This section is dedicated to the physics of the problem through graphical representation of concentration profile. Solution is obtained using Mathematica. Effects of different parameters: squeezing parameter $S$, Magnetic parameter $M$, Radiation parameter $Nr$, nanoparticle volume fraction $\emptyset$, Eckert number $Ec$, and Schmidt Number $Sc$ on concentration are represented through Figures 6.5 – 6.11. Figures 6.12 – 6.15 represent effects of pertinent parameters on Skin friction $C_f$ and Nusselt number $Nu$. It is evident from Figure 6.5 that concentration increases with $S$. It is clear from Figure 6.6 that concentration decreases with increase in nanoparticle volume fraction. Increment in concentration with $M$ is evident from Figure 6.7. Decrease in concentration profile with increasing values of $Sc$ is evident through Figure 6.8. Figure 6.9 shows that concentration can be decreased by considering higher values of $Nt$.

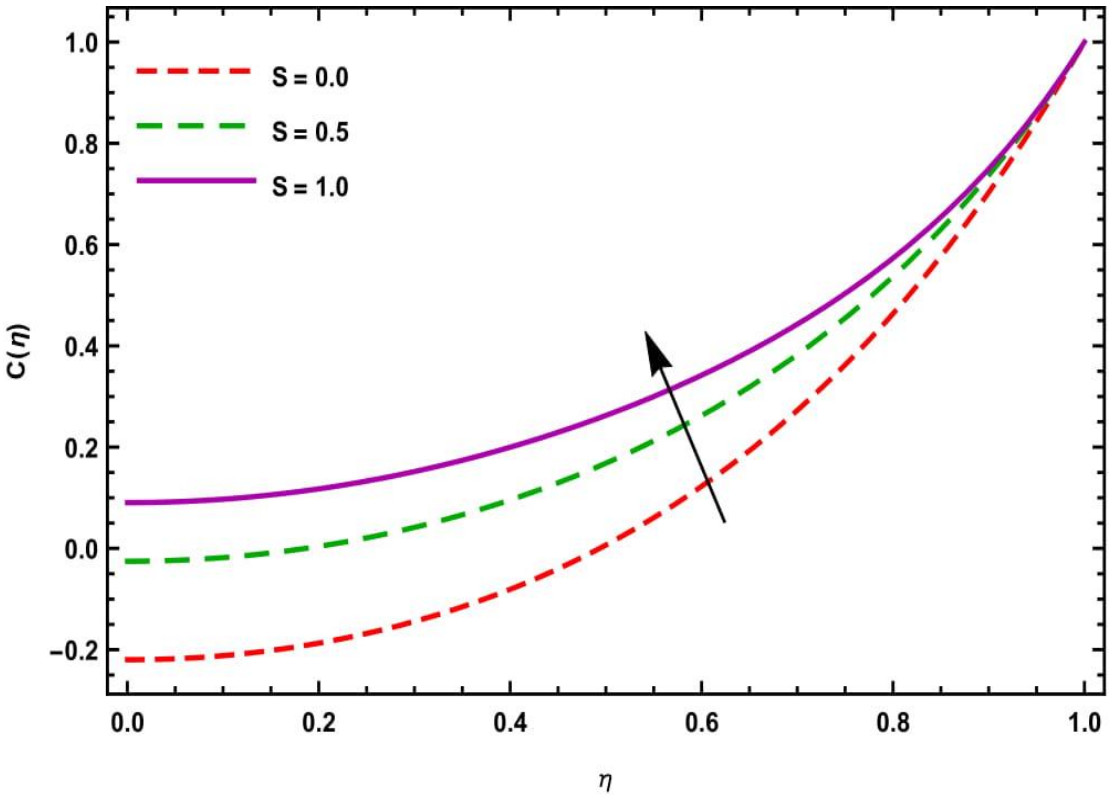


**Figure 6.5:** Concentration profile $C$ for $\eta$ and $S$ at $\phi = 0.02,\ M = 0.5, Nr = 1.0,$ $Pr = 6.2,\ \ Ec = 0.05,\ \delta = 0.15,\ \lambda = 1.2,\ Nb = 0.1,\ Nt = 0.1\ and\ Sc = 0.3.$

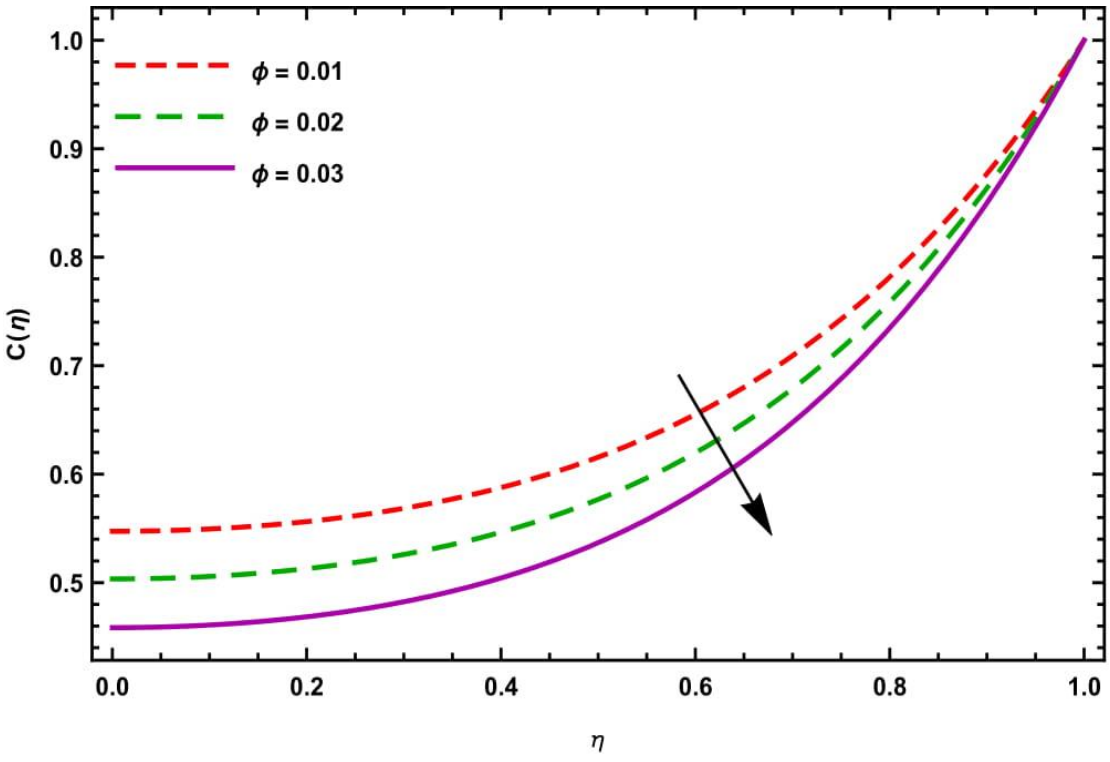


**Figure 6.6:** Concentration profile $C$ for $\eta$ and $\phi$ at $S = 0.3,\ M = 0.5, Nr = 1.0,$ $Pr = 6.2,\ \ Ec = 0.05,\ \delta = 0.15,\ \lambda = 1.2,\ Nb = 0.1,\ Nt = 0.1\ and\ Sc = 0.3.$

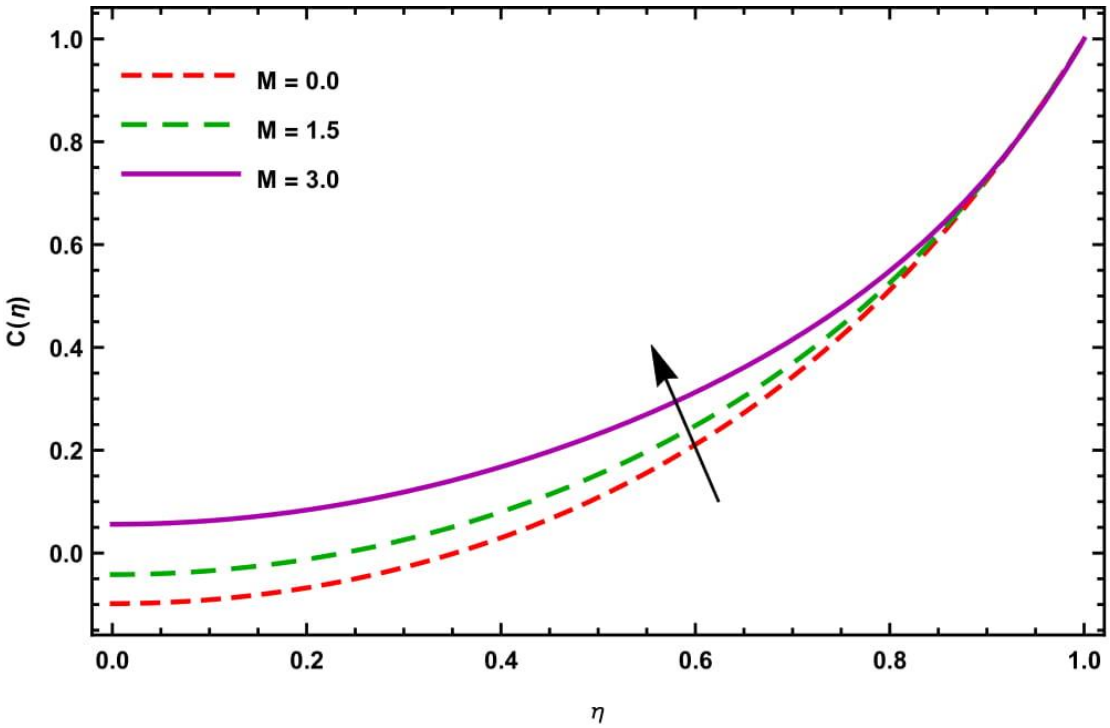


**Figure 6.7:** Concentration profile $C$ for $\eta$ and $M$ at $S = 0.3, \phi = 0.02, Nr = 1.0,$ $Pr = 6.2,\ \ Ec = 0.05,\ \delta = 0.15,\ \lambda = 1.2,\ Nb = 0.1,\ Nt = 0.1\ and\ Sc = 0.3.$

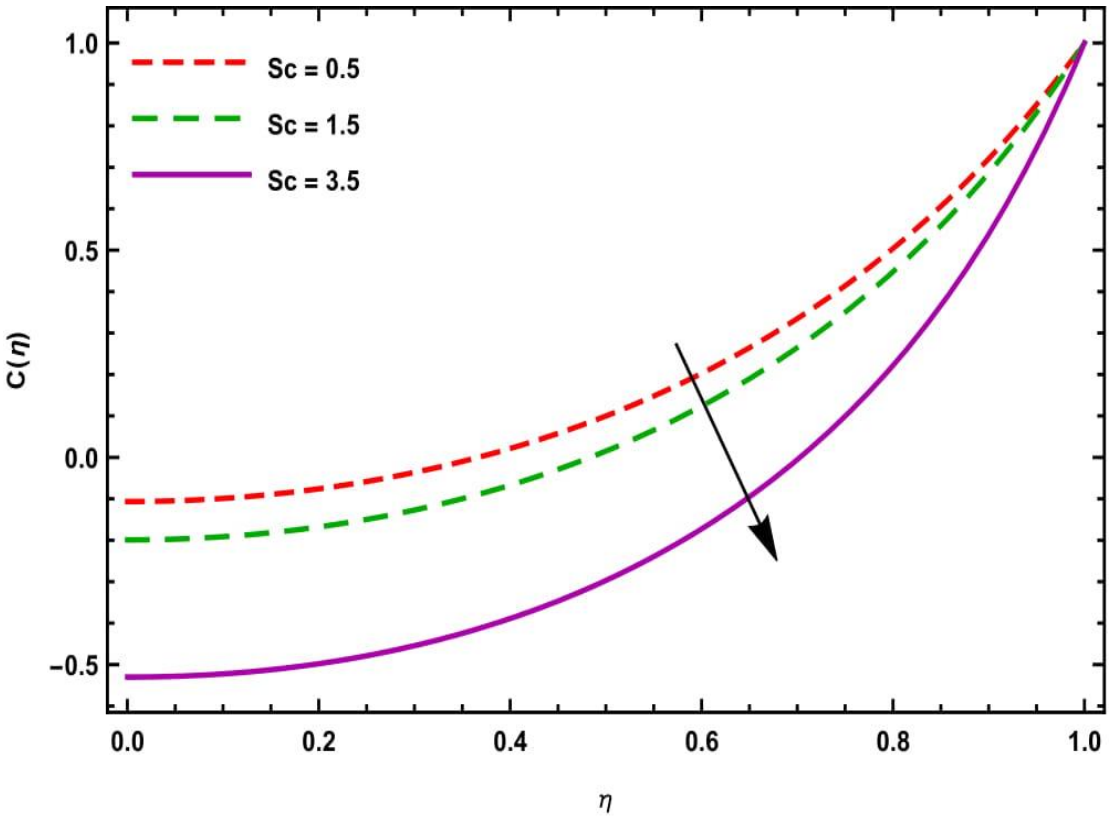


**Figure 6.8:** Concentration profile $C$ for $\eta$ and $Sc$ at $S = 0.3, \phi = 0.02, Nr = 1.0,$ $Pr = 6.2,\ \ Ec = 0.05,\ \delta = 0.15,\ \lambda = 1.2,\ Nb = 0.1,\ Nt = 0.1\ and\ M = 0.5.$

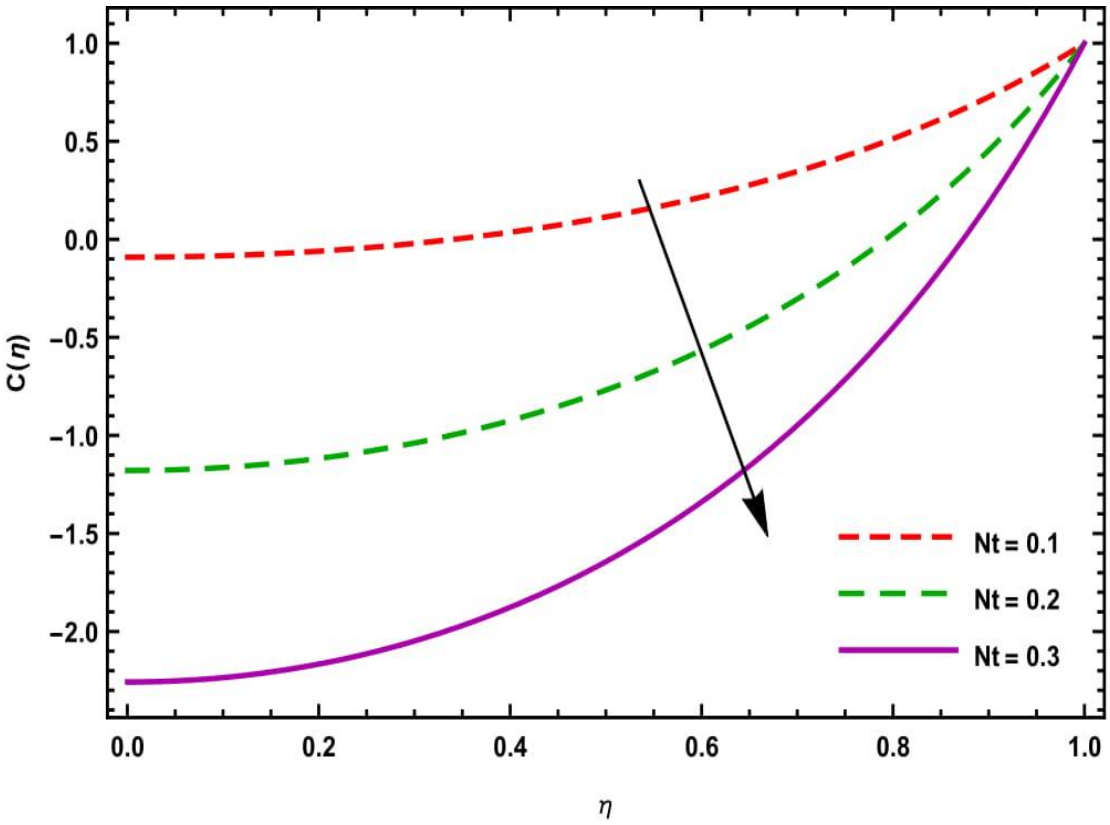


**Figure 6.9:** Concentration profile $C$ for $\eta$ and $Nt$ at $S = 0.3, \phi = 0.02, Nr = 1.0,$ $Pr = 6.2,\ \ Ec = 0.05,\ \delta = 0.15,\ \lambda = 1.2,\ Nb = 0.1,\ Sc = 0.3\ and\ M = 0.5.$

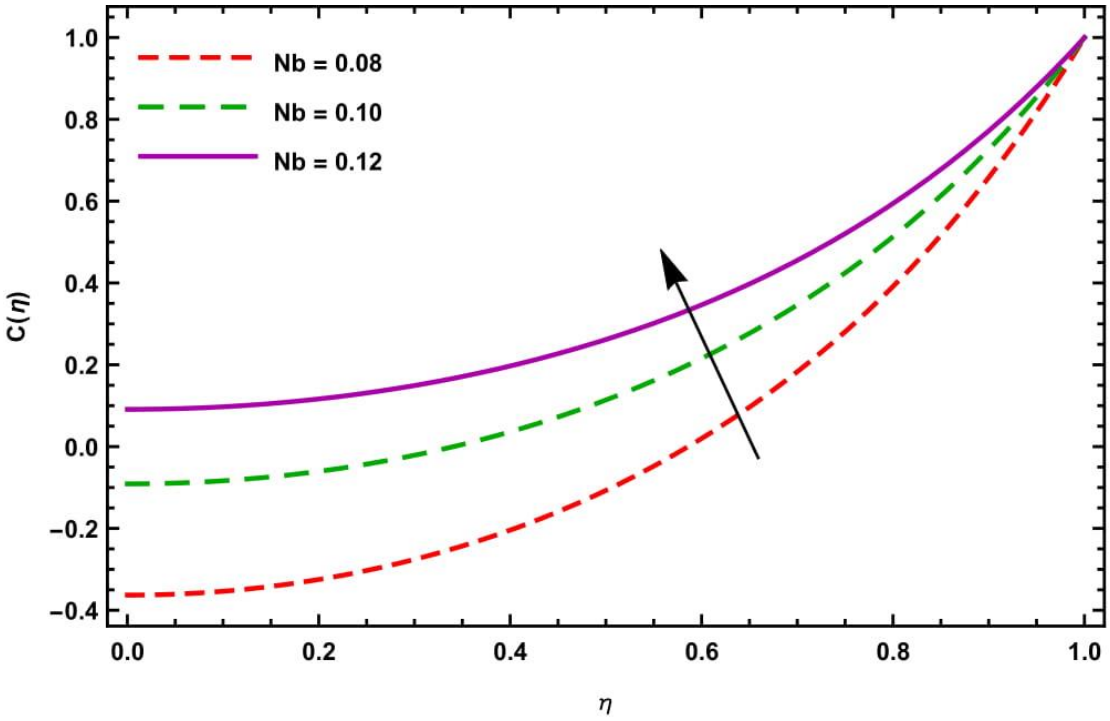


**Figure 6.10:** Concentration profile $C$ for $\eta$ and $Nb$ at $S = 0.3, \phi = 0.02, Nr = 1.0,$ $Nt = 0.1, Ec = 0.05,\ \delta = 0.15,\ \lambda = 1.2,\ Pr = 6.2, Sc = 0.3\ and\ M = 0.5.$

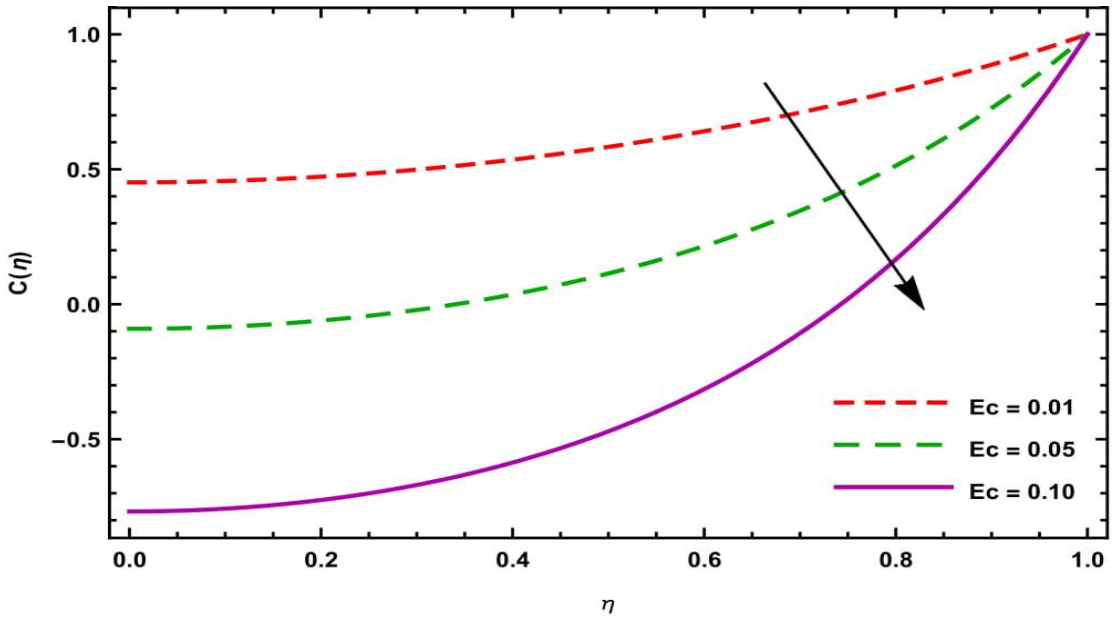


**Figure 6.11:** Concentration profile $C$ for $\eta$ and Ec at $S = 0.3,\ \phi = 0.02, Nb = 0.1,$ $Nt = 0.1, \lambda = 1.2, \mathrm{Nr} = 1.0, \delta = 0.15, Pr = 6.2, Sc = 0.3\ and\ M = 0.5.$

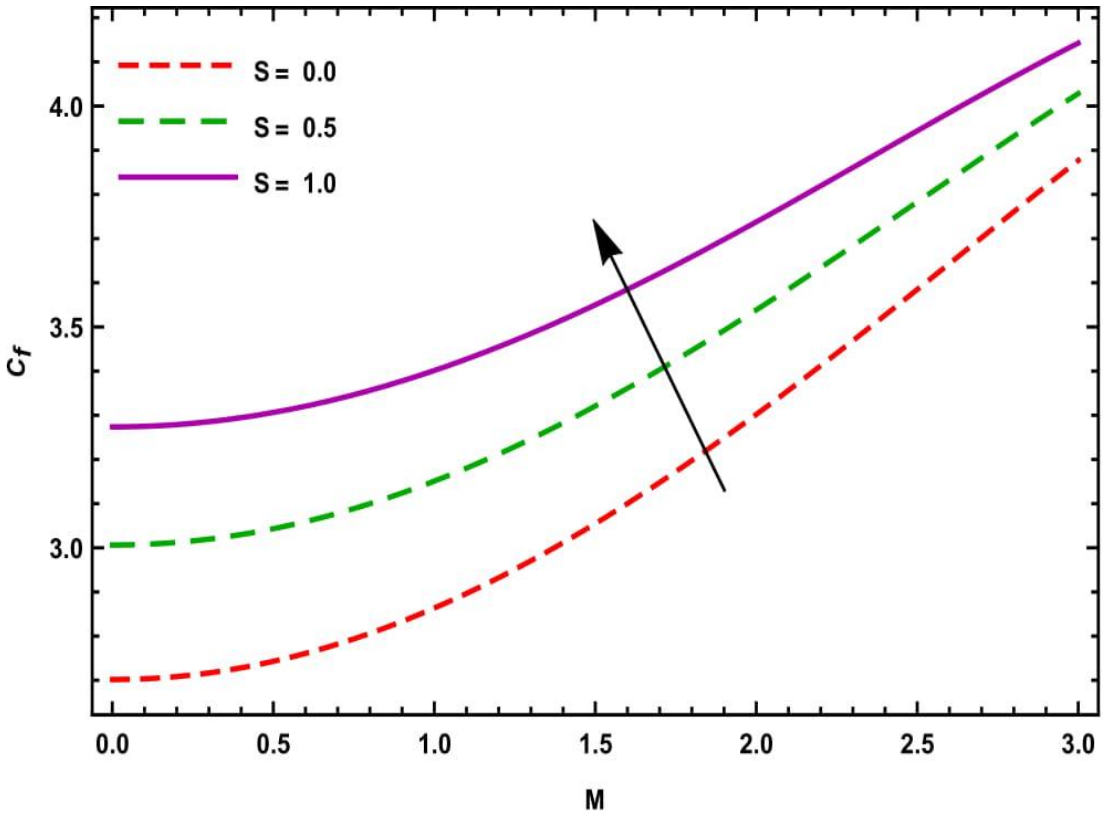


**Figure 6.12:** Effect of magnetic parameter M and S on $C_f$ at $\phi = 0.02, Nr = 1.0,$ $Pr = 6.2, Ec = 0.05,\ \delta = 0.15,\ \lambda = 1.2,\ Nb = 0.1,\ Nt = 0.1\ and\ Sc = 0.3.$

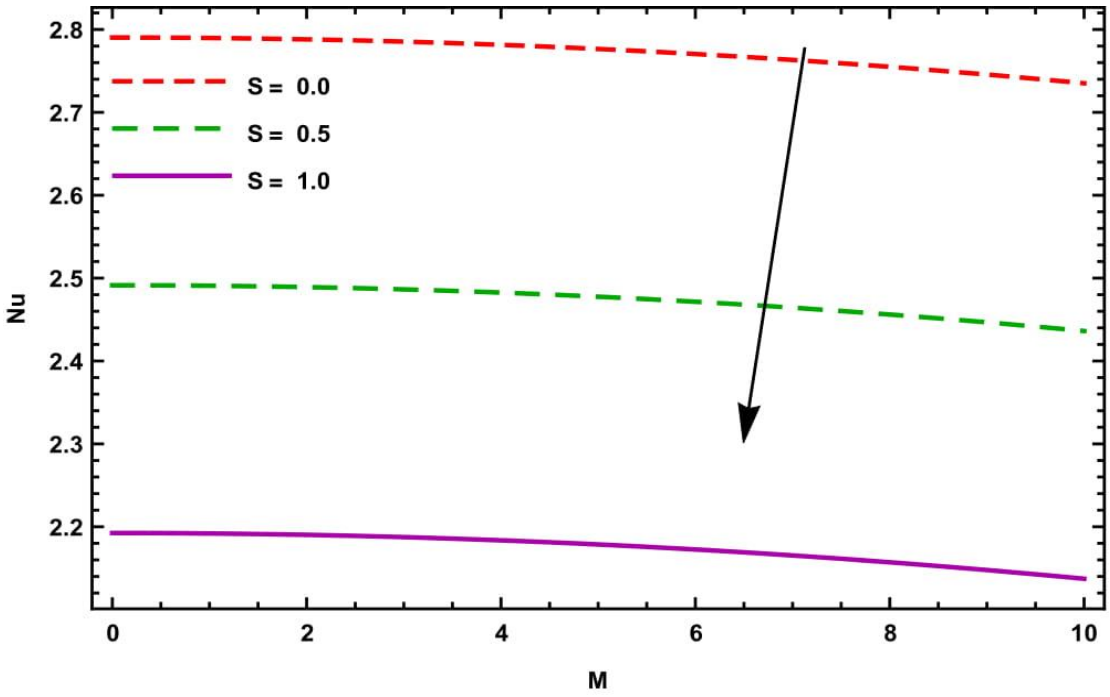


**Figure 6.13:** Effect of magnetic parameter M and S on $Nu$ at $\phi = 0.02,\ Nr = 1.0,$ $Pr = 6.2, Ec = 0.05,\ \delta = 0.15,\ \lambda = 1.2,\ Nb = 0.1,\ Nt = 0.1\ and\ Sc = 0.3.$

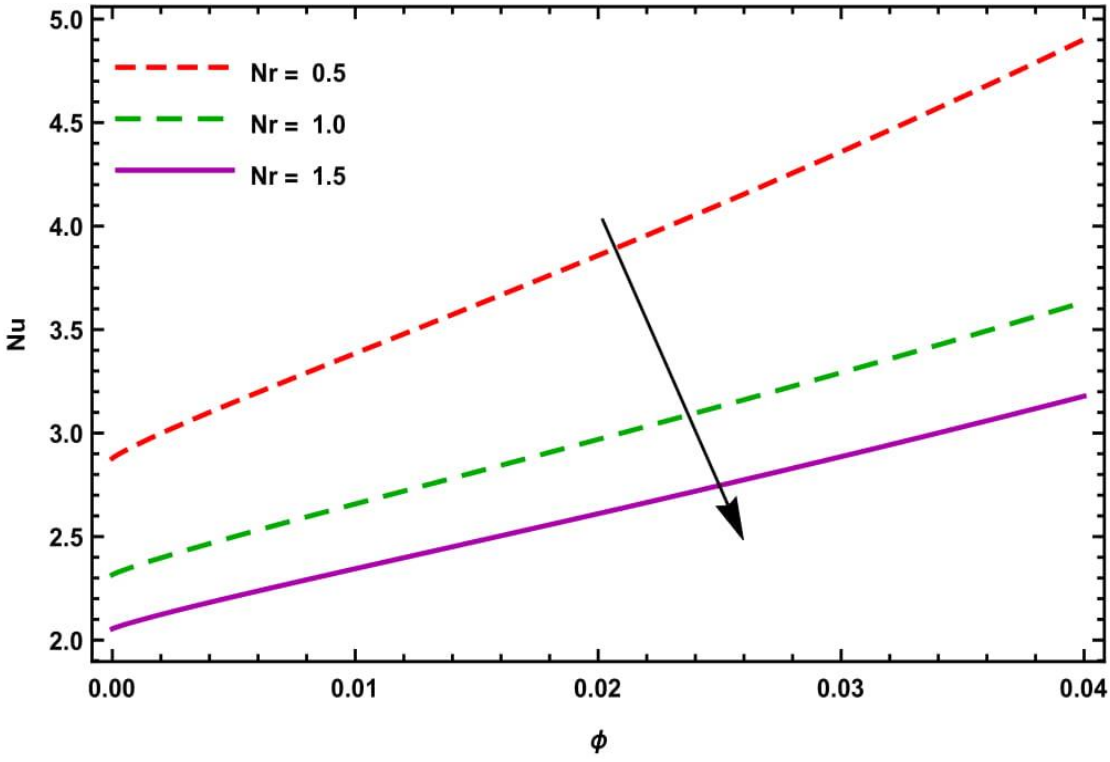


**Figure 6.14:** Effect of nanoparticle volume fraction $\phi$ and $Nr$ on $Nu$ at $M = 0.5,\ S = 0.3,$ $Pr = 6.2, Ec = 0.05,\ \delta = 0.15,\ \lambda = 1.2,\ Nb = 0.1,\ Nt = 0.1\ and\ Sc = 0.3.$

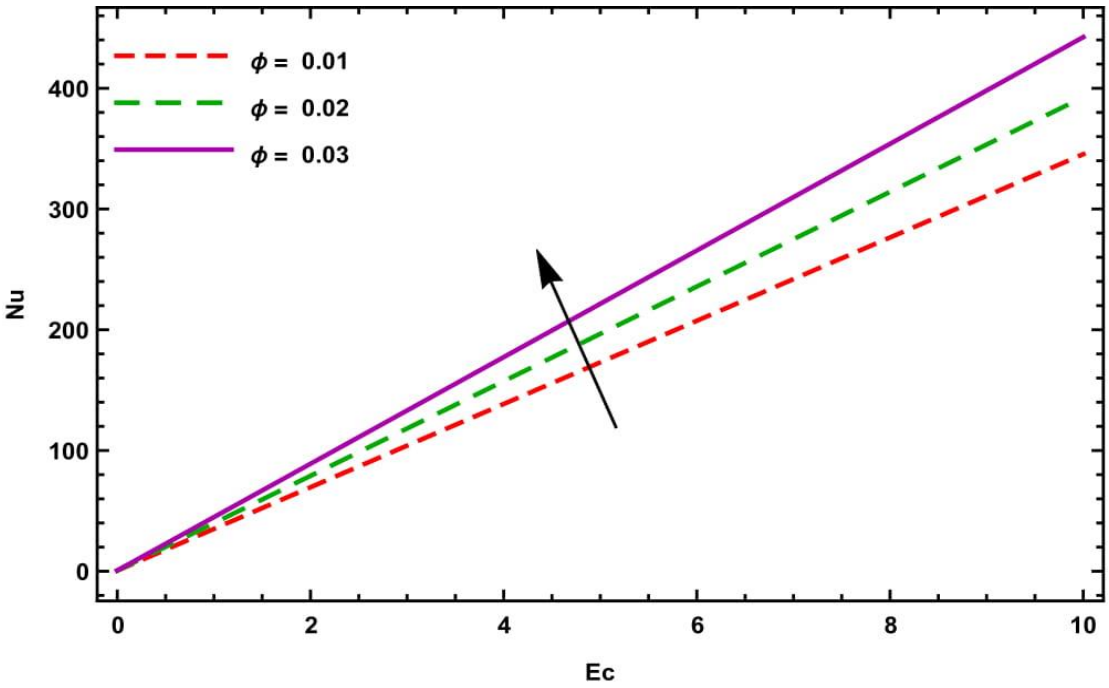


**Figure 6.15:** Effect of Eckert number Ec and $\phi$ on $Nu$ at $M = 0.5,\ Nr = 1.0,\ Pr = 6.2,$ $S = 0.3,\ \delta = 0.15,\ \lambda = 1.2,\ Nb = 0.1,\ Nt = 0.1\ and\ Sc = 0.3.$

Effects of $Nb$ on concentration profile is evident from Figure 6.10. It is observed that concentration increases with increase in $Nb$. Figure 6.11 demonstrates that concentration profile decreases with rise in values of $Ec$. Figure 6.12 shows skin friction for different values of M and $S$. It is seen that, Skin friction increases with increase in either of parameters. Figures 6.13 – 6.15 illustrate effects of different physical parameters on Nusselt Number. It is evident that $\phi$ tends to increase the values of Nusselt number while $S$ and $Nr$ has reverse effect on it.

## 6.6 Conclusion

The most important concluding remarks can be summarized as follows:

- Concentration can be increased by increasing $M$ or $S$.
- Concentration declines with increasing values of $Ec$.
- Skin friction can be reduced by diminishing $S$.
- Nu increases with increase in $\emptyset$ or $Ec$.